FAILURE MECHANICS OF THICK, CURVED, LAMINATED COMPOSITE STRUCTURES

M. Battley[1]*, L. Matheson[1], K. Karumbiah[1], S. Lake[2] and T. Allen[1]

[1] CENTRE FOR ADVANCED MATERIALS MANUFACTURING & DESIGN (CAMMD)
[2] CORE BUILDERS COMPOSITES, WARKWORTH, NZ
• CORRESPONDING AUTHOR: m.battley@auckland.ac.nz

INTRODUCTION

The F50 catamaran is a two-hulled sailing yacht used for the Sail GP international sailing competition. These high-performance yachts use hydrofoils to lift the main hulls out of the water to reduce drag. Two types of hydrofoils are used, C/L shaped forward retractable dagger foils and inverted T shaped rear rudders. The C/L-shaped foils have a vertical hydrofoil section to generate horizontal forces and a single horizontal hydrofoil on the bottom to generate vertical lift. The dagger foils provide the majority of the hydrodynamic lift and hence are a critical load bearing structure. These are manufactured from autoclave cured preimpregnated carbon fibre reinforced epoxy composite laminates and are typically many tens of mm thick.

Through-thickness (radial) stresses occur in the curved corner regions of the hydrofoils between the vertical and horizontal sections of the foils due to the bending moments at the corner regions. These have resulted in delamination damage during service, particularly when an "opening moment" is generated during complex boat handling scenarios. In this research, the structural behaviour and failure mechanics of thick, curved composite laminates was investigated.

The aims of the project were to understand the structural behaviour and failure mechanics of thick, curved composite structures under an 'opening' load scenario and evaluate the capabilities of non-destructive inspection techniques and diagnostic methods such as Acoustic Emission (AE) monitoring to identify manufacturing defects and characterise in-service damage initiation and propagation.

FIGURE 1. SAIL GP F50 SAILING CATAMARAN

STRESS STATES

Numerical and analytical models were developed to investigate the stress states and design the physical specimens for laboratory testing. The specimen geometry was designed such that the peak radial stress would exceed the through-thickness strength of the laminate before in-plane stresses became critical. This was achieved by ensuring a stress ratio of at least 30 between the circumferential and radial stresses. A mean radius of 0.2 m was selected which is within the range of general radii of dagger foils (0.1 – 0.5 m)

Figure 2 presents the effect of specimen thickness on the through thickness (radial) stress, showing how the thinner specimens have significantly high stresses. Figure 3 Show how the radius (R) of curvature affects the radial stress, with much higher stresses for smaller radius. Figure 4 shows a typical through thickness stress distribution.

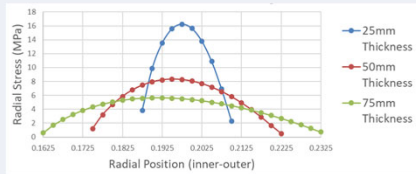

FIGURE 2. EFFECT OF THICKNESS ON RADIAL STRESS DISTRIBUTION THROUGH THICKNESS

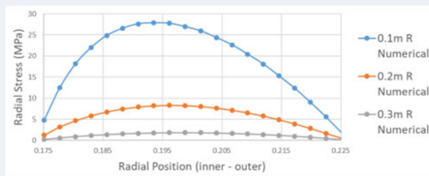

FIGURE 3. EFFECT OF CURVATURE ON RADIAL STRESS DISTRIBUTION THROUGH THICKNESS

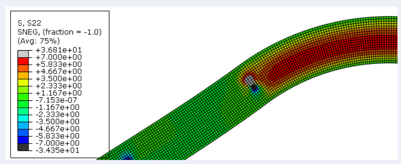

FIGURE 4. THROUGH THICKNESS STRESS DISTRIBUTION

EXPERIMENTAL APPROACH

Specimens were manufactured from a single laminate panel ensuring consistent manufacture parameters for processes such as debulking and curing. A male tool was made with a radius the same as the intended inner radii. Carbon-fibre pre-impregnated laminated specimens were manufactured by hand lamination techniques and autoclave curing, similar to the dagger foil production manufacturing. To ensure adequate consolidation of the laminate stack, a maximum of 20 mm of laminate could be cured at one time. This was achieved through three cures of 56 plies, for a thickness of approximately 16.8 mm for each lamination stage.

Three different samples were produced, Full-Thickness (RF), Large Radii (RL) and Small Radii (RS). The geometry of the three sample sets are detailed in Table 1. Four specimens were manufactured RF and three each for RL and RS. of Figure 5 presents the full thickness RF curved composite specimen.

TABLE 1. CURVED SPECIMEN GEOMETRY

Sample	Thickness (mm)	Width (mm)	Inner Radius (m)	Outer Radius (m)
RF	50	40	0.175	0.225
RL	25	25	0.2	0.225
RS	25	25	0.175	0.2

FIGURE 5. FULL THICKNESS CURVED COMPOSITE SPECIMEN

A four-point bending test fixture (Figure 6) was used to apply monotonic static and cyclic bending loads with a support span of 500 mm and loading span of 250 mm. Through-thickness strains were measured using a resistance strain gauge rosette and Digital image correlation (DIC).

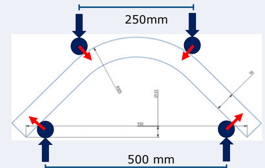

FIGURE 6. LOADING GEOMETRY

DAMAGE DIAGNOSTICS

A review was undertaken of alternative diagnostic methods for characterizing defects and damage in this type of thick laminated structure. Techniques considered included Acoustic Emission (AE) Monitoring during loading, and pre and post-test Non-Destructive Inspection methods such as Computed X-ray Tomography, 2D Radiography, Shearography, Infrared Thermography, Ultrasonic Inspection and Vibration based Modal Analysis. Shearography, Infrared thermography and vibration modal analysis all have proven to have limited applicability in thickness greater than 5 – 10 mm. Computed Tomography has shown to produce useful results, however access to and size of the expensive equipment is limiting to the scanning of dagger foils and not suitable for in-field use.

The two selected techniques were Acoustic Emission Monitoring which has been shown to be useful for characterizing damage initiation and propagation during loading and Phased Array Ultrasonic Inspection which is suitable for thick composite laminates and is practical for manufacturing and in-field inspection. The objective of the diagnostic testing was to observe and characterise as-manufactured defects and the initiation and propagation of failure in the specimens.

The specimens were ultrasound scanned using Olympus Omniscan SX equipment and a RollerFORM phased array transducer prior to testing to evaluate the manufactured quality. Potential defects from manufacture included inclusions, fibre wrinkling, voids, and delamination. During loading AE monitoring was used to identify onset and progression of damage and its location. Ultrasound scanning was then undertaken again after failure.

Cyclic loading protocols were designed to further investigate specific AE events (Figure 7). In this loading scenario, specimens were monotonically loaded to a specific load and fully unloaded. In the next cycle, the load level was increased until a load greater than the previous cycle was reached. Ultrasound scanning was undertaken after critical acoustic emission signals or after completion of each cycle of load to monitor damage accumulation (Figure 8).

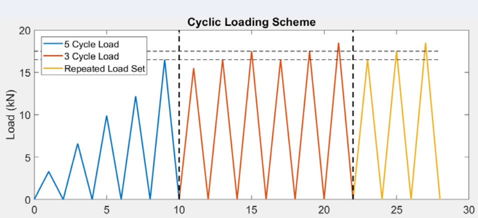

FIGURE 7. CYCLIC LOADING SEQUENCE

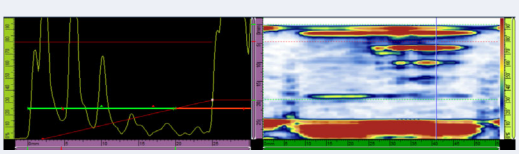

FIGURE 8. TYPICAL ULTRASOUND RESULTS (LEFT: ASCAN, RIGHT B-SCAN)

DAMAGE EVOLUTION

Figure 9 shows Acoustic Emission Counts and Amplitude for the thick specimen RF1. An increase in amplitude of events can be seen up to a point of high amplitude after which the event amplitude drops then increases again before final failure. This general behaviour was also observed in RF2 and RF3. In samples RF1 and RF2 three distinct cluster of high number of events with peak amplitudes between 80-100 dB could be observed. The first group occurs between 15.5 - 16.5 kN (C1), while the second and third occur around 18 kN within 500 N of each other (C2 and C3). The third event occurred with final failure of RF2, and was the last set of signals with a significant amplitude for RF1.

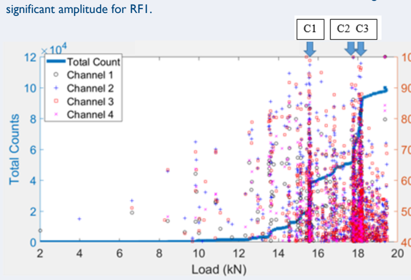

FIGURE 9. DAMAGE EVOLUTION FOR 40MM THICK RF1

Figure 10 shows Acoustic Emission Counts and Amplitude for thinner specimen RS1. This sample showed a progressive non-linear increase of AE count up until final failure. Small steps in AE counts can be observed at 4.9 kN and 5.65 kN however the increase in count is not as significant as those seen in RF1-3. The channel associated with the peak amplitudes varies throughout the loading with channel 4 being the peak at 4.9 kN and channel 2 being the peak at 6.2 kN.

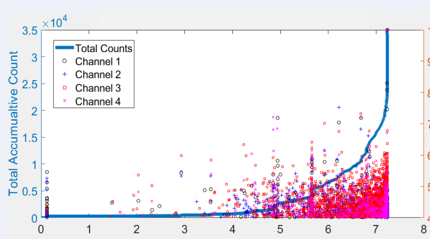

FIGURE 10. DAMAGE EVOLUTION FOR 25MM THICK RS1

Analysis of the AE results also included event frequency, duration, energy release, and event location through time of flight to each sensor. The cyclic loading was also used to investigate the Kaiser and Felicity effects. Ultrasound Inspection (Figure 8) detected delaminations associated with AE events, although not all of these propagated into the final failures.

CONCLUSIONS

- The types of manufacturing related defects and damage onset features that can occur in a thick, curved composite laminate were identified, and the ability of non-destructive test methods to detect them was evaluated.
- The results demonstrated that delamination can be detected within the specimen post-failure. The detection was more effective in the thinner radii samples while the residual specimen stiffness can close the delamination inhibiting detection in the thicker specimen. Multiple manufacture induced features could be detected using ultrasound scanning. These defects can be categorised through the signal shape and signal impedance.
- Acoustic emission and ultrasound inspection did not show conclusive evidence in being able to work together to observe the onset of matrix cracking and delamination. Only one sample, RL2 showed the development of a crack that appears to have propagated into a delamination. Delamination propagation appeared to occur instantaneously for these samples.
- Ultrasound inspection of the thick, laminated composite was possible with damage being identified at significant depths. Post-bonds proved to produce significant signals and potentially hide features.
- The acoustic emission response can be categorised for the different specimens. It was observed that in the static loading tests repeatability in signals occurred. The cyclic behaviour deviated from this, however.
- While it appears as though final failure could be identified through a large duration and energy event there were not enough samples to characterise the data into a failure criterion.
- The Felicity ratio could be applied to observe a propagation in damage leading up to a final failure. The application of this method was limited by the number of significant acoustic events.
- The stress state can be predicted using numerical modelling and was validated using strain gauge recording.
- The relationship between radius and thickness with the stresses generated is similar for the isotropic and orthotropic case. There is a significant role that either of these parameters plays in stress generation especially for thicker and smaller radii samples.
- Failure strength was found to be lower than anticipated. It was observed that existing manufacturing defects had effects on behaviour even if they existed outside the maximum stress region.
- Acoustic Emission responses showed clear onset of matrix cracking followed by progressive damage leading to delamination initiation. The frequency content of the signals suggests delamination as the dominant failure mode.
- Further damage assignment work using clustering methods could be applied in the future.
- These results were used to develop a production quality control protocol for the main dagger foils and inverted T shaped rear rudders that was implemented in the Sail GP manufacturing facilities. This was based on cyclic proof loading of every hydrofoil component in two bending load cases, with Acoustic Emission monitoring and resistance strain gauges.
- This was done after manufacturing and for any components that were repaired after in-service damage. Ultrasound inspection was used to detect and monitor growth of in-service damage prior to repair.

ACKNOWLEDGEMENTS

The authors would like to acknowledge the technical and financial support of Core Builders Composites/Sail GP Technologies, and also scholarship funding through Callaghan Innovation

CAMMD.co.nz